

NORSAR Scientific Report No. 1-87/88

Semiannual Technical Summary

1 April — 30 September 1987

L.B. Loughran (ed.)

Kjeller, December 1987

VII.2 Preliminary tests for surface waves in 2-D structures

Introduction

Surface waves at short periods ($T \leq 20$ s), and especially the Lg crustal surface waves, usually exhibit complex wavetrains. For example, relative amplitudes of the Lg to body-wave phases observed at the NORSAR array were shown to be strongly path-dependent (Kennett et al, 1985), and large transversal motion was observed on Lg-phases produced by explosive sources in the North Sea (Kennett and Mykkeltveit, 1984).

Lateral heterogeneities are thought to be responsible for this complexity, but due to the lack of methods which are available to model surface wave propagation in laterally heterogeneous structures, little of the complex wavetrains has yet been explained. In order to get some further insight into these surface wavetrains, we have initiated a research effort aiming at comparing surface wave recordings at the NORSAR and NORESS arrays with results of numerical modelling, using a coupled mode scheme. The preliminary results presented here do not intend to model a realistic situation, but to check the applicability of the method, and especially to analyze the influence of its two main parameters.

Method

We give here an outline of a coupled local mode method, the details of which can be found in Maupin (1987). It is appropriate for propagation across 2-D structures, the angle of incidence of the waves upon the structure being possibly nonperpendicular to the symmetry direction y of the structure. The wavefield is decomposed into a laterally varying sum of the local modes:

$$\vec{u}(x,y,z,t) = \int_{-\infty}^{+\infty} \int_{-\infty}^{+\infty} \left(\sum_r c_r(x) \vec{u}_r(x,z;\omega,p) \right. \\ \left. \exp(-i \int_0^x k^r(\zeta) d\zeta) \right) e^{-ipy} e^{i\omega t} dp d\omega \quad (1)$$

where \vec{u} is a displacement-stress vector of the elastic wavefield, \vec{u}_r are displacement-stress vectors of the local modes, and $(k^r, p, 0)$ is the local wave vector of the mode r in the cartesian coordinate system (x, y, z) , at the frequency ω .

The lateral heterogeneity introduces a lateral variation of the wave-numbers k^r , as well as energy transfers between modes expressed by lateral variations of the amplitude coefficients c_r . The lateral variations of these two quantities satisfy the equations:

$$\frac{dk^r}{dx} = F_{rr} \quad (2)$$

$$\frac{dc_r}{dx} = \sum_{q \neq r} F_{qr} \frac{1}{(k^q - k^r)} \cdot \exp(i \int_0^x (k^q - k^r) d\zeta) c_q$$

where F_{qr} is an expression involving the local mode displacements and tensions, combined with the elastic coefficients and density in interface terms, and with their lateral derivatives in an integral over depth.

The system (2) is transformed to yield a first-order equation in x for reflection and transmission matrices, which is solved numerically in x using a fourth-order Runge-Kutta scheme.

The method is tested on the continental margin model designed by Badal and Serón (1987) (Fig. VII.2.1) to calculate Love wave transmission by finite element method. We use an integration step in x of 5 km and a variable integration step in z of the form $a^{(n-1)} dz_0$ for the n -th step, with $dz_0 = 0.5$ km and $a = 1.02$. In the following two paragraphs, we investigate the influence on the coupling matrices of the precision with which the local modes are calculated, and of the number of modes used in the representation of the wavefield.

Influence of the number of zones

The local modes \vec{u}^r appear free of lateral differentiation in the expression F_{qr} of equation (2). In order to facilitate their computation, it is thus possible not to calculate them at each integration step in x , but to take them as constant inside zones where the total lateral variation of the structure is small enough for their shape not to vary significantly. The coarser a zoning we define across the laterally heterogeneous structure, the less accurate local displacement functions we use in the calculation of the expression F_{qr} , which in turn result in less accurate coupling matrices and local wavenumbers.

In order to determine how fine the zoning must be, we divide the continental margin of Fig. VII.2.1 into 2, 5 and 10 zones. The coupling equation is integrated with the three different zonings, using the local modes at a period of 20 s, calculated at the center of each zone by a classical Haskell-Dunkin method. The resulting local phase velocities of the Rayleigh wave fundamental mode are shown on Fig. VII.2.2a as a function of x . The phase velocities calculated at the center of each zone by the Haskell-Dunkin method, as well as the local phase velocities calculated in each of the smaller zones using the variational method, are shown on Fig. VII.2.2b for comparison.

The variational method is designed to calculate first-order variations of the phase velocity associated with velocity and density variations as a function of depth, preferably for flat layer boundaries. Equation (2) treats separately the effect on phase velocities of sloping layer boundaries and velocity variations inside the layers. It gives obviously more accurate results than the variational method in this continental margin model, where the slope of the layer boundaries is important.

The accuracy of the phase velocity improves significantly when using 5 zones instead of 2, but remains stable between 5 and 10 zones. The number of zones required to fit a given velocity curve can be foreseen from the linear trend of the integrated phase velocity inside a zone. The proper zoning for a given model and frequency depends on the curvatures of the different mode phase velocity variations. The discrepancy observed between the integrated phase velocity and the zonal phase velocities around $x = 30$ km may be related to a systematic discrepancy between the vertically varying velocity profile and the set of homogeneous layers required by the Haskell-Dunkin method to calculate the zonal phase velocities.

The zoning must be designed to calculate accurately not only the phase velocities, but also the transmission and reflection matrices. Fig. VII.2.3 shows the transmission matrices for the 6 first modes of Rayleigh and Love waves at right angle to the continental margin when the modes are calculated at 20 s period for 2, 5 and 10 zones. The zoning has a negligible influence on the transmission matrices. The reflection matrices are zero whatever the zoning for this model.

When the propagation is not at right angle to the structure, Love and Rayleigh waves are coupled. As the dispersion curves of Love and Rayleigh modes of the same harmonic rank are usually very close and may even cross each other, small relative errors in k produce large errors in $(k^q - k^r)$, leading to a loss of accuracy in the Rayleigh-Love

coupling terms. The accuracy of the phase velocity has therefore a stronger influence on the coupling matrices in that case.

Influence of the mode cut-off

To be complete, the wavefield representation (1) should include all the surface wave modes and body-wave terms, or the infinite set of modes of a structure equivalent to the spherical Earth. For practical reasons, we need to restrict the set of modes to those which have somewhere along the structure a significant energy in the frequency range we are studying. Except in particular cases of well-defined waveguides, the coupling between modes usually decreases gradually with harmonic rank difference and the mode cut-off is often chosen somewhat arbitrarily. Therefore, it is important to know which elements in the coupling matrices are influenced by the drop-off of the higher modes.

Transmission matrices for Love waves crossing the continental margin at right angle were calculated for the 6, 8 and 10 first modes at a period of 10 s (Fig. VII.2.4). The influence of the mode cut-off can essentially be inferred from on the last row and column of the matrices. It is clear for example that the addition of modes 9 and 10 has no significant influence on the transmission matrix of the first 7 modes, including the 6th mode which is very strongly coupled to neighboring modes.

The important point to note here is that the energy of the higher modes not accounted for is mainly fed into the coupling terms of the higher modes of the representation, and not systematically into the diagonal terms. Therefore the cut-off does not produce an upper bias of the self-transmission terms.

Conclusion

We have shown that the coupled-local modes method can be applied to model wave propagation in realistic structures, needing a reasonable amount of lateral zones and local modes to achieve a satisfactory precision in transmission and reflection coefficients. The method has acceptable computing times (typically 10 minutes of CPU time on the IBM 4381/PO2 of NORSAR for the examples displayed in Figs. VII.2.3 and VII.2.4). Next, we intend to apply this method across laterally heterogeneous structures around Scandinavia, like the North Sea Graben and the Tornquist-Teisseyre lineament, and compare the results of the modelling with surface wave data recorded at the NORSAR and NORESS arrays.

V. Maupin, Postdoctorate Fellow

References

- Badal, J. and F.J. Serón (1987): Love wave normally incident at the Atlantic margin of the Iberian Peninsula. *Annales Geophysicae*, 5B, 273-280.
- Kennett, B.L.N., S. Gregersen, S. Mykkeltveit and R. Newmark (1985): Mapping of crustal heterogeneity in the North Sea basin via the propagation of Lg-phases. *Geophys. J.R. astr. Soc.*, 83, 299-306.
- Kennett, B.L.N. and S. Mykkeltveit (1984): Guided wave propagation in laterally varying media. II: Lg waves in north-western Europe. *Geophys. J.R. astr. Soc.*, 79, 257-267.
- Maupin, V. (1987): Surface waves across 2-D structures: a method based on coupled local modes. Submitted to the *Geophys. J.R. astr. Soc.*

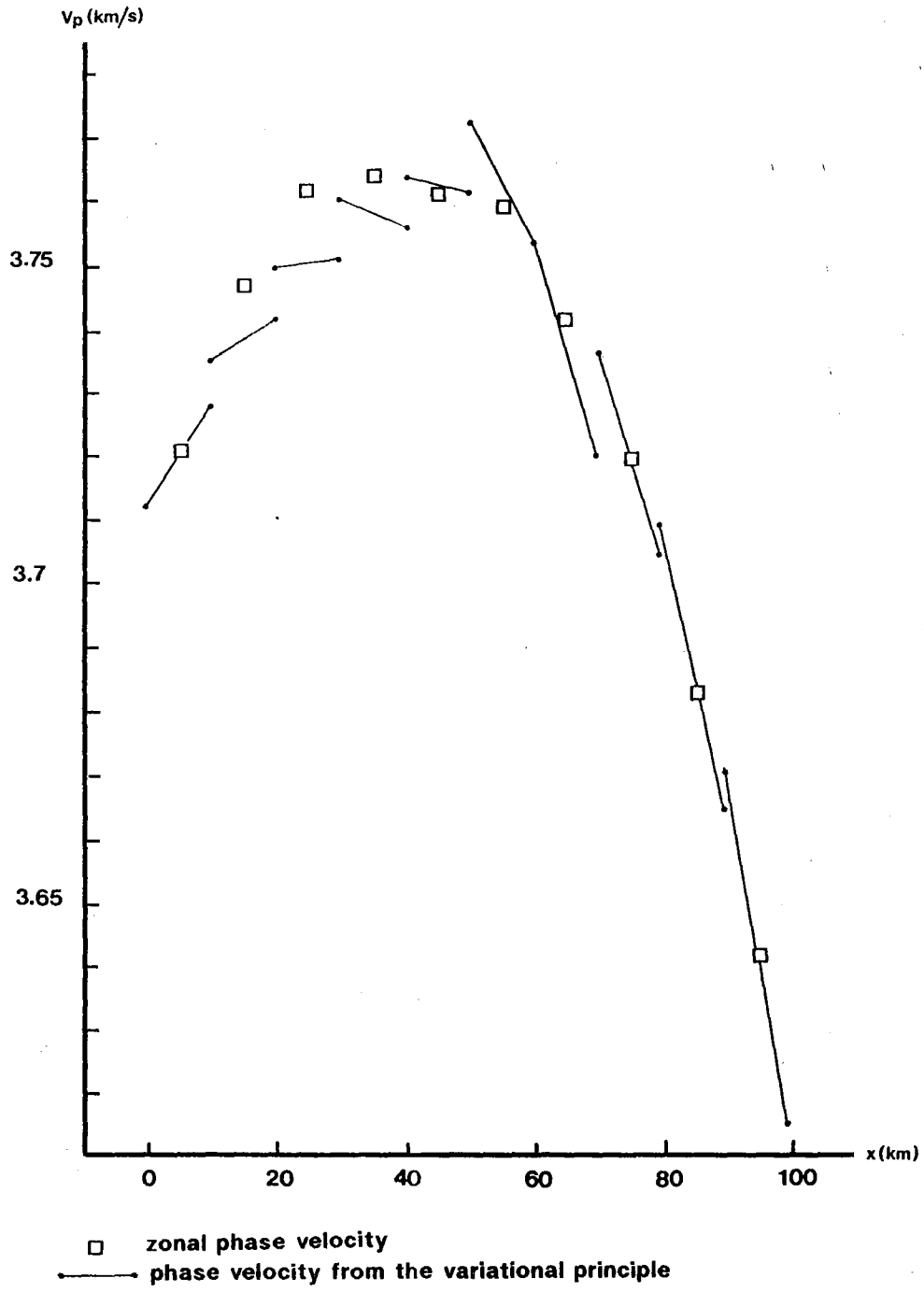


Fig. VII.2.2a

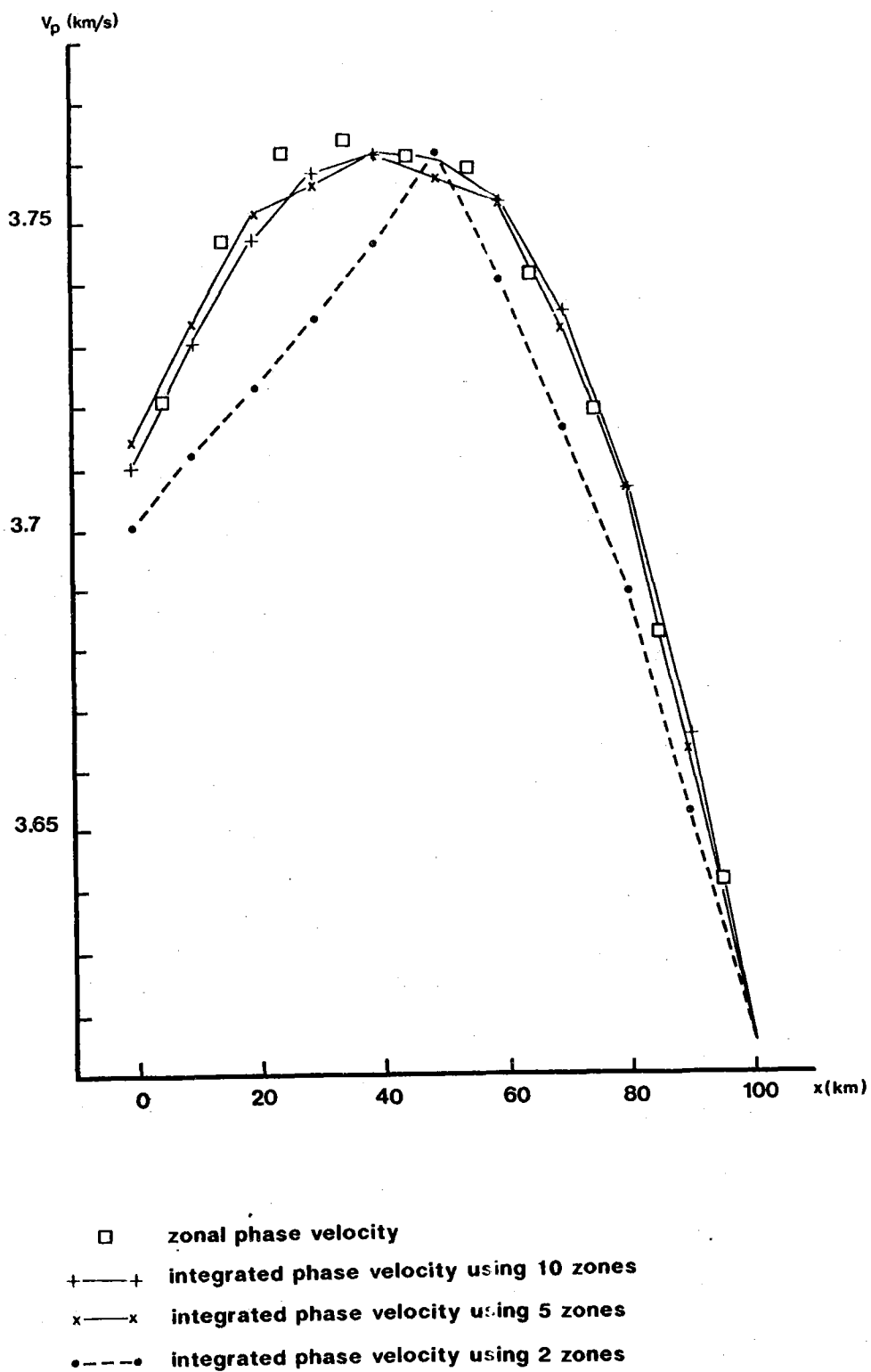


Fig. VII.2.2b

2 zones :

	1	2	3	4	5	6		1	2	3	4	5	6
1	99	3	6	3	5	4		86	39	27	7	9	6
2	6	94	29	9	9	6		46	85	21	3	1	1
3	4	28	93	20	5	6		9	26	79	53	4	4
4	2	13	18	95	17	0		10	14	48	76	38	2
5	3	8	2	15	93	31		11	8	14	31	89	25
6	5	7	8	6	29	94		9	2	2	11	22	96

5 zones :

	1	2	3	4	5	6		1	2	3	4	5	6
1	99	4	7	3	5	4		83	43	28	6	9	7
2	6	94	28	8	8	6		50	84	19	5	1	2
3	5	27	93	22	3	5		8	26	78	55	4	4
4	3	13	19	94	20	0		10	13	49	75	38	2
5	4	7	0	17	91	33		11	8	14	31	88	26
6	5	7	7	7	31	93		11	2	2	12	22	95

10 zones :

	1	2	3	4	5	6		1	2	3	4	5	6
1	99	3	7	3	5	4		84	42	28	6	9	7
2	6	94	28	8	8	6		49	84	20	4	0	2
3	5	27	93	23	3	5		8	27	77	55	4	4
4	3	13	20	94	20	0		10	13	50	75	38	2
5	4	7	0	17	91	33		11	8	14	31	89	26
6	5	7	7	7	32	93		10	2	2	12	22	96

Rayleigh modes

Love modes

Fig. VII.2.3 Transmission matrices in % for the 6 first Rayleigh and Love modes across a continental margin model, at 20 s of period, using 2, 5 and 10 zones. The matrix elements are amplitude transmission coefficients for modes which carry a unit energy flux.

	1	2	3	4	5	6				
1	96	13	14	14	6	4				
2	21	73	59	21	4	2				
3	8	52	35	67	21	27				
4	6	34	65	62	23	7				
5	5	17	17	24	40	84				
6	6	10	18	14	85	44				

	1	2	3	4	5	6	7	8		
1	96	12	14	14	7	5	6	3		
2	20	73	59	21	5	1	1	2		
3	7	52	34	68	24	23	5	3		
4	5	34	65	60	21	7	10	8		
5	5	17	18	21	45	72	38	1		
6	3	6	9	6	58	4	73	30		
7	5	6	12	13	55	52	27	54		
8	8	4	8	12	13	35	48	77		

	1	2	3	4	5	6	7	8	9	10
1	96	12	14	13	7	5	6	4	3	2
2	20	73	59	21	5	0	2	4	3	2
3	6	52	34	68	24	23	6	6	3	2
4	4	33	65	58	21	7	10	15	13	9
5	5	17	18	22	45	72	39	2	2	1
6	3	6	9	7	58	5	71	34	7	1
7	6	6	12	13	55	53	28	52	10	5
8	5	3	5	9	13	31	38	59	60	6
9	5	5	6	9	0	16	28	39	61	58
10	7	7	9	15	3	5	14	25	47	80

Fig. VII.2.4 Transmission matrices in % for the 6, 8 and 10 first Love modes across a continental margin model, at 10 s of period. The matrix elements are amplitude transmission coefficients for modes which carry a unit energy flux.